

# Side-Channel Attacks on Triple Modular Redundancy Schemes

Felipe Almeida, Levent Aksoy, Jaan Raik, *Member, IEEE*, and Samuel Pagliarini, *Member, IEEE*

**Abstract**—The interplay between security and reliability is poorly understood. This paper is the first to show how modular redundancy affects a side-channel attack (SCA). Our counterintuitive findings show that modular redundancy can increase SCA resiliency.

**Index Terms**—triple modular redundancy, side-channel attacks, advanced encryption standard.

## I. INTRODUCTION

As the semiconductor industry pushes the limits of transistor technology in a never ending pursuit of miniaturization, radiation effects have become a serious concern not only for aerospace and military applications, but also for terrestrial applications. Of the many radiation effects an integrated circuit (IC) may suffer from, Single-Event Transients (SETs) and Single-Event Upsets (SEUs) [1] are widely studied. The underlying principle is that a charged particle, upon striking the IC, may cause shifts in voltage levels at combinational or sequential elements, creating SETs or SEUs, respectively.

Over the years, many efficient techniques have been used to mitigate radiation effects [2], often making use of some notion of spatial or temporal redundancy [3]–[7]. Triple Modular Redundancy (TMR), one of the most commonly employed solutions, is a technique that employs three instances of a module and adds a majority voter at their outputs. The scheme, therefore, protects against any single fault in any of the modules. TMR can be deployed with different levels of granularity [6], [7], with diversification [8], and also with approximation [9]. TMR also presents partial protection against multiple faults caused by single-event-induced charge sharing [6].

However, when a fault tolerant circuit is implemented with TMR or a similar technique, its resiliency against security vulnerabilities tends to be overlooked. Recently, the field of Hardware Security has received a lot of attention and defense techniques against various adversaries have been implemented for a range of circuits. Yet, the interplay between security techniques and fault tolerance techniques is still poorly understood. In this paper, our aim is to highlight this interplay by taking an Advanced Encryption Standard (AES) crypto core as a case study. The reliability technique we are concerned with is TMR in its many forms. The security attack we are concerned with is the side-channel attack (SCA). The key-finding of this paper is that **TMR appears to increase the resiliency to SCAs**. Let us now give a brief background on SCAs.

F. Almeida, L. Aksoy, J. Raik and S. Pagliarini are with the Centre for Hardware Security - Department of Computer Systems - Tallinn University of Technology, Ehitajate tee 5, 12616 Tallinn, Estonia (e-mail: {felipe.almeida, levent.aksoy, jaan.raik, samuel.pagliarini}@taltech.ee.)

## II. BACKGROUND ON SIDE-CHANNEL ATTACKS

In an SCA, an adversary collects, in a non-invasive way, leakage data that can be used to discover private information and/or to gain privileged access to a circuit [10]. Power consumption, timing, electromagnetic emanations, and even sound are examples of side-channels that can and have been exploited. Based on the analysis of this residual information, it is possible to perform an attack that breaks security assumptions. In this paper, our focus is on SCAs that exploit power traces as a form of leakage. These power-based SCAs can be categorized in three groups: i) Simple Power Analysis (SPA); ii) Differential Power Analysis (DPA); iii) Correlation Power Analysis (CPA). SPA is a simple graph analysis of the power trace consumption over time. DPA uses statistical analyses at different times to correlate power consumption measurements with functionality. CPA uses a Hamming weight power model method [11] for a more powerful attack.

Crypto cores have been the typical targets of SCAs. In principle, the math behind the crypto function is sound and cannot be broken by formal cryptanalysis. However, the physical realization of the crypto function gives adversaries powerful information.

In [12], an evaluation of the sensitivity to DPA of several protected versions of an AES circuit is discussed. In [13], a power analysis attack on an AES hardware implementation is presented and an SCA is mounted on a physical device with the aid of a simple setup (scope and probes). The attack utilizes the power consumption during the first two clock cycles of the AES computation to discover the secret key. The reason for which the attack works is that in the considered AES implementation, an XOR operation between the plaintext and the secret key is executed in the first clock cycle. The result of this operation is saved in an *intermediate register* in the second clock cycle. The adversary can devise a **hypothetical power model** to account for changes in the value of the intermediate register, i.e., the adversary can use bit changes in this register as a proxy for the behavior of the power consumption of the entire AES circuit. Even further, by simulation means, the adversary can analyse all possible changes the register might have, e.g., toggle count, in a cycle-accurate manner. This type of modelling is widely utilized in SCAs to discover the secret key in a device that implements AES.

This paper focuses on power consumption information leakage to discover the secret key in an AES crypto core. We assume the AES core is meant for a high-dependability application and therefore, TMR has been applied to it. We also assume the adversary has access to power traces of

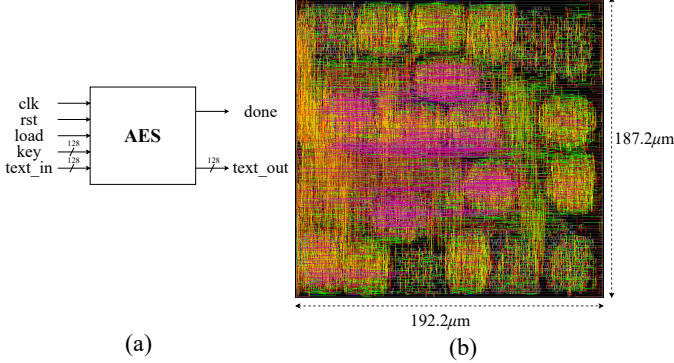


Fig. 1: (a) Block diagram of the AES circuit; (b) its layout.

the circuit under attack. For this reason, the attack is more realistic for terrestrial applications. Furthermore, our approach emulates a physical attack by obtaining detailed power traces from physical synthesis. In practice, a real attack is more complicated because the environment, board, and package become sources of noise that have to be accounted for. For more details on attack feasibility, we direct the readers to [13].

### III. AES CRYPTO CORE IMPLEMENTATION AND SIDE-CHANNEL POWER ANALYSIS ATTACK

A 128-bit AES crypto core from [14] is used to perform a side-channel power analysis attack. Fig. 1(a) shows its block diagram. The AES circuit takes a 128-bit secret key (*key*) and a plaintext (*text\_in*) as inputs and produces a ciphertext as an output (*text\_out*).

The AES crypto core is implemented in a standard design flow which includes the synthesis of Verilog Hardware Description Language (HDL) codes of the AES circuit into a gate-level netlist. Synthesis is performed by Cadence Genus with a commercial 65 nm standard cell library. The target frequency is 500 MHz. Physical synthesis, including floor-planning, placement, and routing, is performed by Cadence Innovus. Fig. 1(b) presents the layout of the AES crypto core. This is our baseline implementation and is referred as single AES in the experiments that follow.

The flow of our side-channel power analysis attack is illustrated in Fig. 2. Compared to the traditional design flow, extra steps were included to enable our attack. To cope with the exponential size of all possible keys i.e.,  $2^{128}$ , the simulation data is obtained for  $L$ -bits of the 128-bit secret key, where  $L$  is set to 8 in our experiments. Therefore, a netlist generated after logic synthesis is instantiated 256 times in a testbench, one instance for each possible 8-bit key. As a result of simulation, we obtain the *simulation data set* which consists of the number of bit changes in the *intermediate register* under all possible values of the  $L$ -bit key.

Another output of the simulation is a Value Change Dump (VCD) file, which annotates any changes in any signals of the design, along with the time of the change. The VCD file is used as an input of another extra step in our design flow, i.e., the power vector profile. Cadence Innovus reads the VCD file and generates a vector-based dynamic power report for any time window of interest. This power estimation is a good representation of the power dissipation of the fabricated

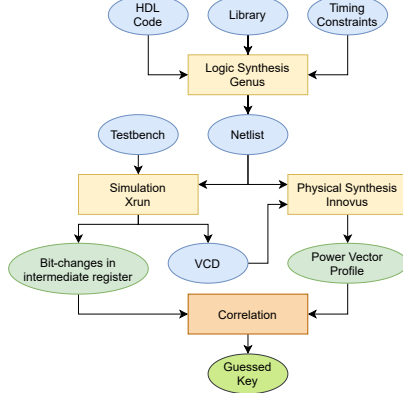


Fig. 2: Side-channel power analysis attack flow.

chip because it takes into account parasitic information from extraction and representative input patterns from simulation<sup>1</sup>. We obtain the *power data set* which is computed as the difference of the power dissipation values of the AES crypto core in the first and second clock cycles as described in [13]. Note that 1000 randomly generated plaintexts were used to obtain these simulation and power data sets.

Finally, for each possible key, the Pearson Correlation Coefficient (PCC) is computed between the simulation data and the power data set, and the one that leads to the maximum PCC value is determined to be the guessed key. In the text and results that follow, without loss of generality, we perform attacks on 8 bits of the secret key at a time. The same attack can be repeated 16 times to uncover the entire 128-bit secret key. The design flow is automated using Python scripting and the runtime to discover the 8 bits of the secret key in an AES is approximately 2 hours for 1000 plaintext inputs. The majority of the runtime is spent doing power analysis and the correlation calculation is much simpler in comparison.

Fig. 3(a) presents the PCC value for each possible key guess for the 8 Most Significant Bits (MSBs) of the secret key. In this experiment, we set 8 MSBs of the secret key to 222. Note that the attack has been successful as the highest PCC value is also 222. We note that the minimum number of plaintexts required to find the correct value of 8 MSBs of the secret key is 698, as shown in Fig. 3(b). Note that at that point, when 698 plaintexts have been correlated, the green line becomes the one with the highest PCC. As more plaintexts are considered, the correlation tends to become clearer.

### IV. SIDE-CHANNEL ATTACKS ON TMR SCHEMES

In order to demonstrate the SCA resiliency of a TMR'd circuit, the same AES crypto core was designed under a coarse-grain TMR architecture. Two different physical designs, called AES\_TMR and AES\_TMR\_MACRO, were considered. In the AES\_TMR design, the physical synthesis tool is allowed to perform independent optimizations in the three instances if applicable. In the AES\_TMR\_MACRO design, each instance in

<sup>1</sup>For readers with IC design background, we clarify that we utilize the Voltus power analysis engine of Innovus with VCD and Standard Delay Format (SDF) files. We ask the tool to generate a power estimation at every 1ns to oversample the 500 MHz frequency of operation of the circuit. This matches the capability of an adversary equipped with a typical oscilloscope.

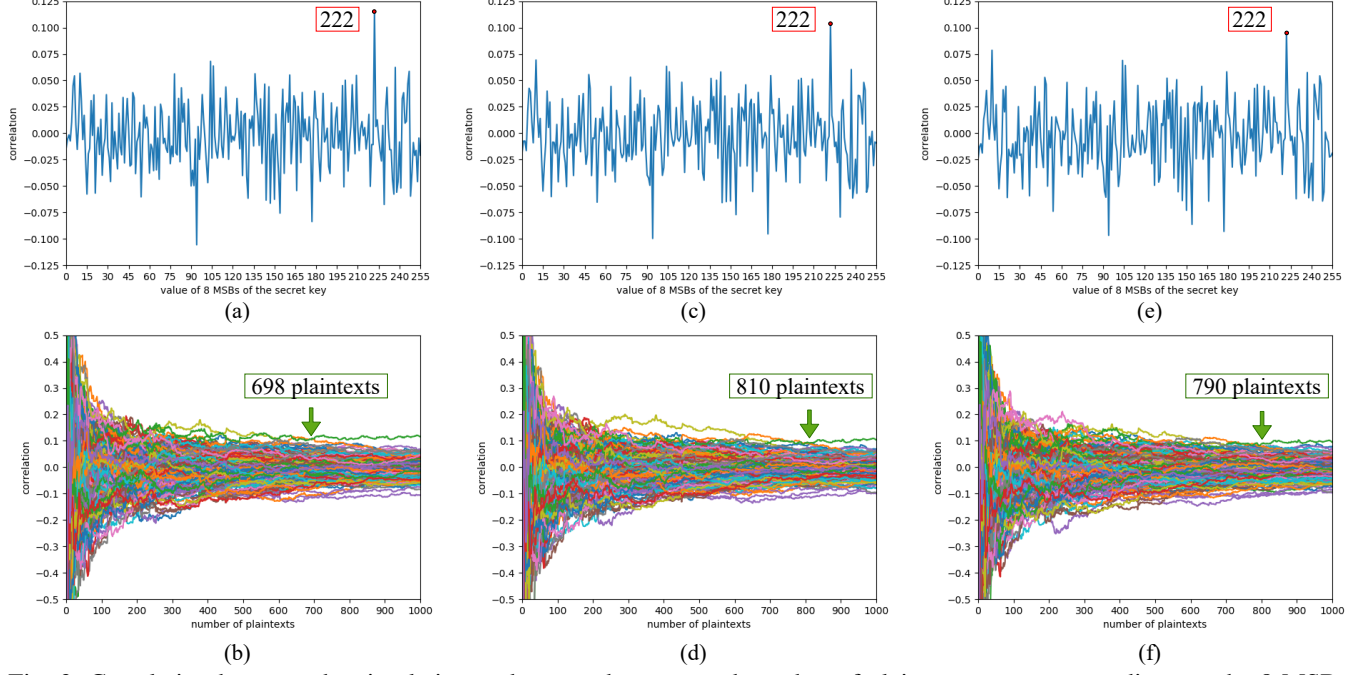


Fig. 3: Correlation between the simulation and power data sets and number of plaintexts necessary to discover the 8 MSBs of the secret key when they were set to 222: (a)-(b) single AES, (c)-(d) AES\_TMR, and (e)-(f) AES\_TMR\_MACRO.

the TMR architecture is purposefully made identical: all cells and all metal routing lines are the same for all three instances.

Fig. 4(a) shows the amoeba and physical layout views of the AES\_TMR design which has three instances of the AES crypto core with different numbers of cells, placement, and routing. Figure 4(b) presents the amoeba and physical layout views of the AES\_TMR\_MACRO design which has identical instances. Note that both TMR designs have the same timing constraints, core area, and pinouts for the sake of a fair comparison.

The SCA described in Section III is also applied to these TMR architectures. Fig. 3(c) presents the PCC values for all possible key guesses under the AES\_TMR architecture, where the maximum value, which is 222, denotes the correctly guessed key. Note that it is the same as the one found in the single AES crypto core, meaning that the attack has been successful. Moreover, Fig. 3(d) shows the number of plaintexts necessary to determine the secret key under the AES\_TMR architecture, i.e., 810. Note that the AES\_TMR circuit needs a larger number of plaintexts to discover the secret key when compared to the single AES crypto core. This result is, at first glance, not logical. After all, the TRM'd circuit is performing the same computation three times, which intuitively leads us to believe it would leak 3x as much information. We hypothesize that the TMR instances are acting as noise sources to one another, making the attack's convergence slightly harder.

Fig. 3(e) presents the PCC values for all possible key guesses under the AES\_TMR\_MACRO architecture. The guessed key is the same as obtained under the single AES crypto core and AES\_TMR circuit. Fig. 3(f) shows the number of plaintexts necessary to determine the secret key under the AES\_TMR\_MACRO architecture, i.e., 790. Note that the required number of plaintexts is higher than the one found in the single AES crypto core, but slightly smaller than the one

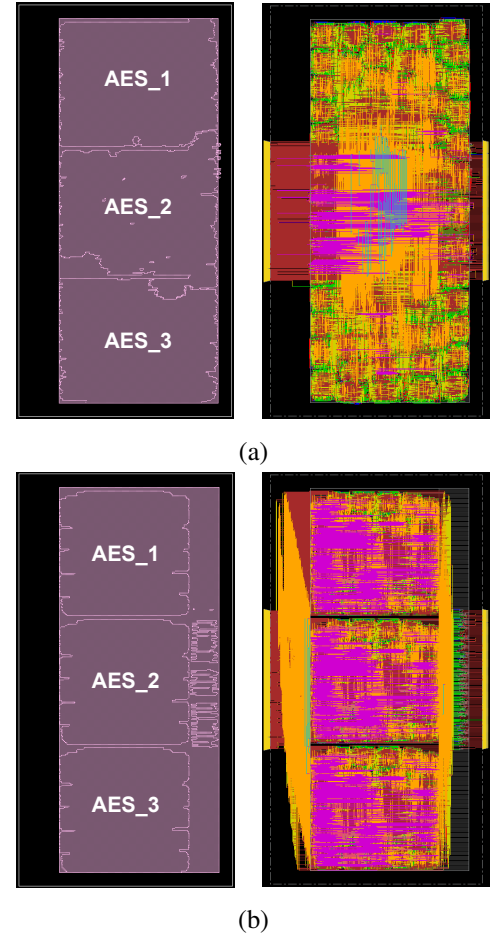


Fig. 4: Amoeba views and layouts of TMR architectures: (a) AES\_TMR; (b) AES\_TMR\_MACRO.

TABLE I: Details on each AES\_TMR\_DIVERSE instance.

AES Instance	#gates	Static Power (μW)	Dynamic Power (mW)
Baseline	9826	0.3472	15.84
Clock Gated	9853	0.3472	15.12
Retimed	10187	0.3511	16.73

computed in the AES\_TMR circuit. Here, we clarify that the plaintexts are generated by a pseudorandom function, so any differences in SCA resiliency can be attributed to the circuit itself and not to the value of the chosen plaintexts.

In summary, the results from Fig. 3 indicate that manipulating the level of disparity between the TMR instances can be used as a knob to tune SCA resiliency. We took this idea one step further by implementing the AES crypto core under another TMR architecture, called AES\_TMR\_DIVERSE, where each instance is physically and structurally different, but all instances remain functionally equivalent. To do so, we performed the physical synthesis of the same TMR'd AES crypto core with three different gate-level netlists. The first one is our baseline AES, the second one is obtained after applying the clock gating technique which is used to reduce power dissipation in parts of the circuit that are not being switched (and therefore, has an impact on SCA resiliency), and the third one is obtained after performing the retiming technique which moves the relative location of latches and registers, primarily to improve performance. Table I shows the design details of each AES instance in terms of the number of gates, static and dynamic power.

Fig. 5 shows that our SCA was unable to discover the secret key for the AES\_TMR\_DIVERSE version, even when 2000 random plaintexts were considered. Note that in this experiment, the utilized key, i.e., 222, remains the same, but the guessed key was 48. The correct key leads to the second highest PCC value. These results clearly show that the use of a diverse TMR architecture can increase the resiliency to SCAs. Therefore, under TMR architectures, an implementation with diverse circuits provides not only reliability, but also security when compared to a traditional TMR implementation.

## V. CONCLUSION

This paper demonstrated how a fault tolerance technique interferes with security, more precisely with the SCA resiliency. Even further, it showed how a TMR scheme with diversity can be leveraged to improve said resiliency. As it stands, the use of reliability techniques in order to increase the security of a circuit is largely unexplored territory. The possibilities for future avenues of research are plenty, including the study of redundancy schemes other than TMR.

## ACKNOWLEDGMENT

This work has been partially conducted in the project “ICT programme” which was supported by the European Union through the ESF. It was also partially supported by the Estonian research council grant MOBERC35.

## REFERENCES

[1] R. C. Baumann, “Radiation-Induced Soft Errors in Advanced Semiconductor Technologies,” *IEEE Transactions on Device and Materials Reliability*, vol. 5, no. 3, pp. 305–316, 2005.

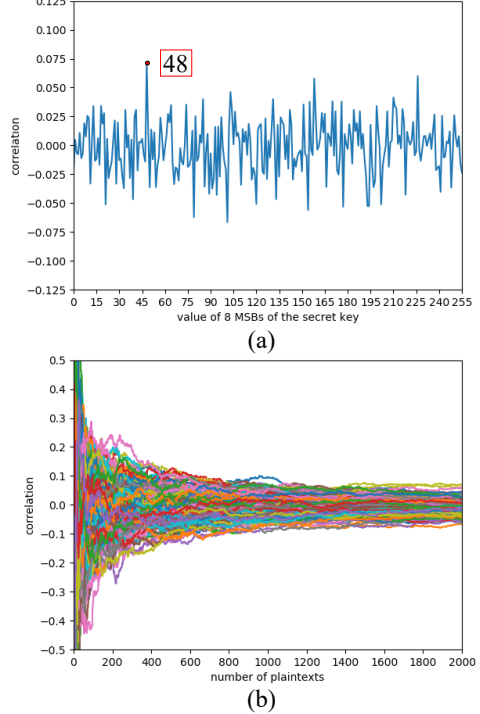


Fig. 5: SCA on the AES\_TMR\_DIVERSE circuit: (a) correlation between the simulation and power data sets; (b) number of plaintexts required to find 8 MSBs of the secret key.

[2] S. Kasap, E. Weber Wächter, X. Zhai, S. Ehsan, and K. McDonald-Maier, “Survey of Soft Error Mitigation Techniques Applied to LEON3 Soft Processors on SRAM-Based FPGAs,” *IEEE Access*, vol. 8, pp. 28 646–28 658, 2020.

[3] M. Nicolaidis, “Time Redundancy based Soft-Error Tolerance to Rescue Nanometer Technologies,” in *IEEE VLSI Test Symposium*, 1999, pp. 86–94.

[4] S. Nascimento Pagliarini, L. Alves De Barros Naviner, and J.-F. Naviner, “Selective Hardening Methodology Concerning Multiple Faults,” in *IEEE Nuclear and Space Radiation Effects Conference*, 2012.

[5] H. Jeon and M. Annavaram, “Warped-DMR: Light-Weight Error Detection for GPGPU,” in *IEEE/ACM International Symposium on Microarchitecture*, 2012, pp. 37–47.

[6] F. Almeida *et al.*, “Single-Event-Induced Charge Sharing Effects in TMR with Different Levels of Granularity,” in *Radiation and Its Effects on Components and Systems (RADECS)*, 2012, pp. 1–7.

[7] S. Pagliarini *et al.*, “Evaluating Architectural, Redundancy, and Implementation Strategies for Radiation Hardening of FinFET Integrated Circuits,” *IEEE Transactions on Nuclear Science*, pp. 1–1, 2021.

[8] S. Mitra, N. R. Saxena, and E. J. McCluskey, “A Design Diversity Metric and Reliability Analysis for Redundant Systems,” in *International Test Conference*, 1999, pp. 662–671.

[9] I. A. C. Gomes *et al.*, “Methodology for Achieving Best Trade-off of Area and Fault Masking Coverage in ATMR,” in *Latin American Test Workshop*, 2014, pp. 1–6.

[10] F.-X. Standaert, “Introduction to Side-Channel Attacks,” in *Secure integrated circuits and systems*. Springer, 2010, pp. 27–42.

[11] S. Mangard, E. Oswald, and T. Popp, *Power Analysis Attacks: Revealing the Secrets of Smart Cards*. Springer-Verlag, 2007.

[12] V. Maingot and R. Leveugle, “Influence of Error Detecting or Correcting Codes on the Sensitivity to DPA of an AES S-box,” in *International Conference on Signals, Circuits and Systems*, 2009, pp. 1–5.

[13] S. B. Ors, F. Gurkaynak, E. Oswald, and B. Preneel, “Power-Analysis Attack on an ASIC AES Implementation,” in *International Conference on Information Technology: Coding and Computing*, 2004, pp. 546–552.

[14] “AES (Rijndael) IP Core,” [https://opencores.org/projects/aes\\_core](https://opencores.org/projects/aes_core), accessed: 2020-12-15.